

Geology

January 2014, Volume 42, Issue 1, Pages 63-66

<http://dx.doi.org/10.1130/G34801.1>

© 2013 Geological Society of America

Archimer
<http://archimer.ifremer.fr>

Fluid flow regimes and growth of a giant pockmark

Yann Marcon¹, H el ene Ondr eas², Heiko Sahling¹, Gerhard Bohrmann¹ and Karine Olu³

¹ MARUM, University of Bremen, Leobener Str., 28359 Bremen, Germany

² IFREMER, Centre de Bretagne, REM/GM, 29280 Plouzan e, France

³ IFREMER, Centre de Bretagne, REM/EEP, 29280 Plouzan e, France

Abstract:

Pockmarks are seafloor depressions commonly associated with fluid escape from the seabed and are believed to contribute noticeably to the transfer of methane into the ocean and ultimately into the atmosphere. They occur in many different areas and geological contexts, and vary greatly in size and shape. Nevertheless, the mechanisms of pockmark growth are still largely unclear. Still, seabed methane emissions contribute to the global carbon budget, and understanding such processes is critical to constrain future quantifications of seabed methane release at local and global scales. The giant Regab pockmark (9 42.6' E, 5 47.8' S), located at 3160 m water depth near the Congo deep-sea channel (offshore southwestern Africa), was investigated with state-of-the-art mapping devices mounted on IFREMER's (French Research Institute for Exploitation of the Sea) remotely operated vehicle (ROV) *Victor 6000*. ROV-borne micro-bathymetry and backscatter data of the entire structure, a high-resolution photo-mosaic covering 105,000 m² of the most active area, sidescan mapping of gas emissions, and maps of faunal distribution as well as of carbonate crust occurrence are combined to provide an unprecedented detailed view of a giant pockmark. All data sets suggest that the pockmark is composed of two very distinctive zones in terms of seepage intensity. We postulate that these zones are the surface expression of two fluid flow regimes in the subsurface: focused flow through a fractured medium and diffuse flow through a porous medium. We conclude that the growth of giant pockmarks is controlled by self-sealing processes and lateral spreading of rising fluids. In particular, partial redirection of fluids through fractures in the sediments can drive the pockmark growth in preferential directions.

1. Introduction

Pockmarks are seafloor depressions considered to be the surficial expressions of fluid seepage processes, as well as mud volcanoes or gas hydrate pingoes (Judd and Hovland, 2007; S eri e et al., 2012). However, pockmark morphologies, sizes and densities vary greatly, suggesting that the term "pockmark" is loosely constrained and applies to a broad range of seafloor features (King and MacLean, 1970; Hovland et al., 2002; Judd and Hovland, 2007; Gay et al., 2007).

The shape of a pockmark is the result of local conditions and the processes involved in the formation and growth of pockmarks are likely to vary between settings. Several formation mechanisms have been proposed that involve either slow and continuous processes (Hovland et al., 1984; Harrington, 1985; Sultan et al., 2010) or more rapid and sudden events (MacDonald et al., 1994; Hovland et al., 2005). All the different hypotheses confirm that several processes could apply and that the main

mechanisms involved in the formation and growth of pockmarks remain largely unclear. A better knowledge of these processes is crucial to strengthen our understanding of the dynamics of methane release from the seabed into the ocean.

In this study we present for the first time the results of high-resolution acoustic and optical surveys of the giant Regab pockmark in the lower Congo basin. Surveys were conducted using the Ifremer's remotely operated vehicle (ROV) Victor 6000 during the West African Cold Seeps (WACS) cruise on the RV Pourquoi Pas? in January-February 2011. The data set is fully

47 comprehensive and includes in particular ROV-borne micro-bathymetry and backscatter maps of
48 the entire pockmark together with detailed sidescan-based mapping of seafloor gas emissions.
49 This is completed by a 105,000 m²-large high-resolution photo-mosaic and fauna mapping of the
50 most populated and active area of the pockmark in terms of seepage intensity.

51 To date, such a comprehensive data set of a pockmark feature is unique and gives
52 unprecedented insights on the detailed morphology of complex pockmarks. In particular, the
53 results provide valuable clues to decipher the functioning of giant pockmarks, which are
54 discussed in this study.

55 **STUDY AREA**

56 The Regab pockmark is located on the Gabon-Congo-Angola margin ~10 km north of the
57 Congo channel at ~3160 m water depth (Ondréas et al., 2005). In this area, muddy hemipelagic
58 sediments cover turbiditic channel/levee bodies of the Congo fan (Droz et al., 1996; Gay et al.,
59 2003). Seismic data show that the pockmark is linked to a deep palaeochannel/levee system that
60 could act as reservoir for the seeping fluids. Advecting fluids are enriched in methane of
61 biogenic origin (Charlou et al., 2004) and sustain an abundant population of chemosynthetic
62 fauna (Olu-Le Roy et al., 2007) within the pockmark. Crusts of authigenic carbonates are
63 extensive (Ondréas et al., 2005; Pierre and Fouquet, 2007) and widespread presence of shallow
64 gas hydrates was inferred from seafloor observations and sediment cores (Charlou et al., 2004;
65 Olu-Le Roy et al., 2007; Pierre et al., 2012).

66 **DATA AND METHODS**

67 Bathymetry data were acquired with a multibeam echosounder (MBES) Reson Seabat
68 7125 running at 400 kHz. The main survey was conducted from 30 m altitude over a 1.2 km²-
69 large area and allowed to map the entire pockmark. An additional survey was conducted from 8

70 m altitude over a 0.175 km²-large subarea of the pockmark. The data was processed with
71 CARAIBES (Le Gal and Edy, 1997) and the final bathymetry and backscatter maps include both
72 data sets with a 25 cm resolution.

73 Imagery data were acquired simultaneously to the second bathymetry survey with the
74 Victor 6000's high sensitivity OTUS photo-camera, and the photomosaic was constructed using
75 the ROV navigation with LAPM Tool (Marcon et al., 2013a). Therefore, an excellent match of
76 the photomosaic onto the bathymetry was obtained. The mosaic was used to map the carbonate
77 precipitates and the fauna distribution. Mapped fauna include siboglinid polychaetes
78 (tubeworms), bathymodiolid mussels and vesicomid clams.

79 Seabed gas emissions in the water column were mapped using the CARIS program to
80 visualize the sidescan data. Sidescan data allowed us to identify the presence of gas in the water
81 column as far as 30 m on each side of the ROV. Due to the dense track line spacing, 86% of the
82 pockmark was mapped. Finally, the presence of gas emissions and outcropping hydrates on the
83 seafloor was confirmed using dive videos.

84 **RESULTS**

85 **Bathymetry**

86 The bathymetry (Fig. 1) shows that the pockmark is a large elliptical structure with
87 diameters ranging between 700 and 950 m. It stretches in the N70 direction along an elongated
88 feature, possibly related to a fracture. Elongated appendices can be observed in several places at
89 the edge of the pockmark. The largest of these occur in the northeastern side and seem to be
90 extensions of the N70 fracture expression. The pockmark boundary shows a sharp edge in the
91 northeastern half, and becomes softer toward the southwestern side. The bathymetry also reveals

92 that Regab is composed of numerous (>1000) rounded depressions, or sub-pockmarks, of various
93 sizes (from less than 5 m to 100 m in diameter) and depths (from 0.5 to 15 m).

94 Those depressions are not randomly distributed and two zones can be clearly
95 distinguished (Fig. 1): zone 1 is composed of relatively large (>20 m) and deep (>3 m) sub-
96 pockmarks, and is characterized by a very rugged surface and the presence of carbonate
97 elevations and slabs; zone 2 has a smoother appearance but is scattered by more than a thousand
98 very small (<5 m) to medium-sized (up to 60 m) and shallow (<3 m) pits, also known as unit
99 pockmarks.

100 **Backscatter and Gas Plumes**

101 The signal reflectivity and gas plume distribution show a very characteristic pattern over
102 the pockmark area (Fig. 1). Zone 1 is almost entirely characterized by high-backscatter
103 reflectivity areas. The largest of them is located around the N70 longitudinal feature identified on
104 the bathymetry; it stretches up to and along the eastern edge of Regab. Two additional areas of
105 high backscatter occur precisely on the boundary of the pockmark, respectively on the northern
106 and southern edges; they are associated with distinct and relatively large sub-pockmarks (80–100
107 m in diameter). Zone 2 has a comparatively low-backscatter signature, but is scattered by a
108 myriad of high-reflectivity anomalies of various sizes (up to 50 m in width) and shapes; these
109 anomalies are consistently located within the numerous shallow unit pockmarks identified from
110 the bathymetry. Vice versa, zone 2 unit pockmarks are always associated with high-reflectivity
111 anomalies. Gas emissions occurred exclusively within the largest high-reflectivity area of zone 1.

112 **OTUS and Video Imagery**

113 The faunal and carbonate mapping from the photomosaic reveals a clear segregation
114 between zones 1 and 2, and a clear causal link with backscatter data (Fig. 2).

115 The rugged morphology of zone 1 is shaped by massive carbonate crusts that form thick
116 elevations around sediment-covered depressions. Gas hydrates occur at the surface in several
117 places (Fig. 1) under carbonate crusts. Near the most active areas in terms of gas emissions,
118 carbonate elevations host abundant mussel and tubeworm populations (Fig. 1–2). Generally,
119 mussel beds are located closer to active gas emissions and in areas of disturbed seafloor, where
120 carbonate crusts seem broken or displaced. Clams are generally distributed in sediment-covered
121 areas of negative relief, but rarely within the deepest depressions of zone 1. Conversely,
122 carbonate crusts, mussels and tubeworms are never observed in zone 2, and the imagery data
123 (photomosaic + dive videos) only reveals soft sediments and clams presence. However, the clam
124 distribution in zone 2 is very distinctive and shows that clams are only present in the center of
125 the unit pockmarks, precisely where the zone 2 high reflectivity anomalies occur (Fig. 2).

126 **DISCUSSION**

127 Previous studies showed that the activity at Regab is linked to the presence of a vertical
128 chimney under the pockmark that is rooted into a palaeo-channel (Ondréas et al., 2005; Gay et
129 al., 2006b) and that the advection of fluid through the gas hydrate stability zone is possibly
130 related to a fault (Gay et al., 2006a). Such interpretation is supported by the elliptical shape of
131 the pockmark and the linear feature evidenced from the bathymetry (Fig. 1). However, although
132 a fracture is likely the main feature controlling the fluid expulsion pattern at Regab, the new
133 high-resolution data revealed two very distinctive zones within the pockmark. These two zones
134 show striking differences and are clearly the expressions of very distinct fluid flow regimes and
135 formation mechanisms.

136 **Zone 1: Intense and Focused Fluid Flow**

137 Thick carbonate elevations, rich fauna and intense gas venting are clear indications for
138 high, focused and long-term seepage activity. First, the abundance of thick crusts of authigenic
139 carbonates at the surface suggests that the anaerobic oxidation of methane (AOM) occurs close
140 to the sediment surface (Aloisi et al., 2002) and has been active for a long period of time (Luff
141 and Wallmann, 2003). A shallow AOM front would therefore indicate an intense upward flux of
142 methane from below (Borowski et al., 1999). Next, patterns in the distribution of mussels and
143 tubeworms (Olu-Le Roy et al., 2007 and Figure 2b-c) indicate that the chemical fluxes are
144 heterogeneous across the zone. In particular, mussels and gas emissions were often observed
145 together. Marcon et al. (2013b) showed that mussel occurrence at Regab reflect areas of intense
146 fluid flow, where chemical supply is locally high. Finally, the faunal distribution (Ondréas et al.,
147 2005), the backscatter signal and the overall shape of zone 1 show a strong correlation with the
148 N70 axis identified from the bathymetry. It is likely that such discontinuity provides the main
149 pathways for focused fluid flow in this zone.

150 The formation of zone 1 topography is not yet fully understood but seafloor observations
151 showed that gas emissions and outcropping hydrates occur in areas of broken crusts or of
152 displaced blocs; such features are evidence for catastrophic events, and are likely related to
153 sudden release of pressured free gas from under the crusts (Hovland et al., 2005) and to rafting of
154 gas hydrates deposits (MacDonald et al., 1994).

155 **Zone 2: Diffuse and Homogeneous Fluid Flow**

156 Carbonates, gas escape and hard substratum fauna were not observed in zone 2. Instead,
157 hundreds of small and medium shallow sub-pockmarks populated by clams scatter the zone (Fig.
158 1–2). We postulate that the relatively smooth surface of zone 2 is the expression of a more
159 diffuse and uniform fluid flow pattern than in zone 1. This is supported by previous works in the

160 Congo basin that correlated the distribution of clams to transient and low seepage activity areas
161 (Olu-Le Roy et al., 2007; Sahling et al., 2008; Marcon et al., 2013b).

162 The formation of those sub-pockmarks could be related to various mechanisms such as:
163 sediment lifting by ascending gas (Hovland et al., 1984), pore fluid drainage (Harrington, 1985;
164 Hovland et al., 2010), rafting of hydrate clumps (MacDonald et al., 1994), or hydrate dissolution
165 (Sultan et al., 2010). A mechanism involving free gas escape in this zone is, however, not
166 supported by the gas emission mapping. In addition, mechanisms involving the presence of
167 shallow gas hydrate deposits are not supported by backscatter data and the observed scarcity of
168 faunal communities (Fig. 1–2), which suggests low seepage activity. However, pore fluid
169 advection does occur at Regab, with rates up to 2.3 mm/a at the western edge of the pockmark
170 (Chaduteau et al., 2009). This favors the models by Harrington (1985) and Hovland et al. (2010),
171 according to which advecting pore water is retained in fine sediments until it is released due to
172 water or gas-triggered pressure buildup. Subsequent sediment winnowing and water drainage
173 ultimately leads to the formation of pits, or unit pockmarks, at the surface.

174 **Possible Mechanisms Controlling the Pockmark Growth**

175 We propose that self-sealing processes and subsequent fluid flow redirection control the
176 pockmark growth (Fig. 3). By causing sediment permeability to decrease, the formation of
177 authigenic carbonates may ultimately form a natural seal for rising fluids (Hovland, 2002).
178 Assuming non-decreasing seepage intensity, a pore-pressure increase would lead excess fluids to
179 spread laterally until sufficient pathways to the sediment surface become available and that
180 uniform flow at hydrostatic pressure is restored. This is similar to the concept of ‘shortest and
181 most permeable vertical pathway’ used to explain the migration of petroleum fluids in rocks and
182 sediments (Mackenzie and Quigley, 1988; Floodgate and Judd, 1992).

183 Redirected fluids may transit as diffuse flow through non-fractured porous sediments or
184 as focused flow along sediment discontinuities. Regab provides evidences for both: mainly
185 focused flow in zone 1 and diffuse flow in zone 2. Results suggest that rising fluids in zone 1
186 were partly redirected through fractures or discontinuities within the sediments, thus leading the
187 pockmark growth into the N70 preferential direction. In the absence of similar preferential fluid
188 pathways, fluid flow in zone 2 spreads over a relatively large area and reaches the surface in a
189 more isotropic way and with a lower intensity than in zone 1.

190 **CONCLUSION**

191 This is the first study to present such a high resolution and comprehensive mapping data
192 set of an entire giant complex pockmark. It demonstrates that current modern techniques exist
193 that allow for detailed and large-scale investigations of the deep-seafloor. The value of such
194 comprehensive data sets goes beyond the mere production of high quality maps. By giving full
195 sight of the area of study it allows getting a deeper understanding of the system and the long-
196 term processes involved. In this study, it allowed identifying zones with distinct fluid flow
197 regimes, and constraining growth mechanisms for giant pockmarks. These findings on pockmark
198 dynamics constitute a base model to orientate future work and constrain assessments of seabed
199 methane fluxes at giant pockmarks.

200 **ACKNOWLEDGMENTS**

201 We would like to thank the captain and crew of RV Pourquoi Pas? and ROV Victor
202 6000. Also thanks to Olivier Soubigou for his help onboard, to Alain Normand for processing
203 the micro-bathymetry, and to James Collins for proofreading the manuscript. This work was
204 supported by the Ifremer and by SENSEnet, a Marie Curie Initial Training Network (ITN)

205 funded by the European Commission 7th Framework Programme, Contract No. PITN-GA-
206 2009-237868.

207 **REFERENCES CITED**

- 208 Aloisi, G., Bouloubassi, I., Heijs, S.K., Pancost, R.D., Pierre, C., Sinninghe Damsté, J.S.,
209 Gottschal, J.C., Forney, L.J., and Rouchy, J.M., 2002, CH₄-consuming microorganisms and
210 the formation of carbonate crusts at cold seeps: *Earth and Planetary Science Letters*, v. 203,
211 p. 195–203, doi:10.1016/S0012-821X(02)00878-6.
- 212 Borowski, W.S., Paull, C.K., and Ussler, W., III, 1999, Global and local variations of interstitial
213 sulfate gradients in deep-water, continental margin sediments: Sensitivity to underlying
214 methane and gas hydrates: *Marine Geology*, v. 159, no. 1–4, p. 131–154,
215 doi:10.1016/S0025-3227(99)00004-3.
- 216 Chaduteau, C., Jean-Baptiste, P., Fourré, E., Charlou, J.L., and Donval, J.P., 2009, Helium
217 transport in sediment pore fluids of the Congo-Angola margin: *Geochemistry Geophysics*
218 *Geosystems*, v. 10, Q01002, doi:10.1029/2007GC001897.
- 219 Charlou, J.L., Donval, J.P., Fouquet, Y., Ondréas, H., Knoery, J., Cochonat, P., Levaché, D.,
220 Poirier, Y., Jean-Baptiste, P., Fourré, E., and Chazallon, B., 2004, Physical and chemical
221 characterization of gas hydrates and associated methane plumes in the Congo–Angola Basin:
222 *Chemical Geology*, v. 205, p. 405–425, doi:10.1016/j.chemgeo.2003.12.033.
- 223 Droz, L., Rigaut, F., Cochonat, P., and Tofani, R., 1996, Morphology and recent evolution of the
224 Zaire turbidite system (Gulf of Guinea): *Geological Society of America Bulletin*, v. 108,
225 p. 253–269, doi:10.1130/0016-7606(1996)108<0253:MAREOT>2.3.CO;2.
- 226 Floodgate, G.D., and Judd, A.G., 1992, The origins of shallow gas: *Continental Shelf Research*,
227 v. 12, p. 1145–1156, doi:10.1016/0278-4343(92)90075-U.

- 228 Gay, A., Lopez, M., Cochonat, P., Sultan, N., Cauquil, E., and Brigaud, F., 2003, Sinuous
229 pockmark belt as indicator of a shallow buried turbiditic channel on the lower slope of the
230 Congo basin, West African margin: Geological Society of London Special Publication 216,
231 p. 173–189, doi:10.1144/GSL.SP.2003.216.01.12.
- 232 Gay, A., Lopez, M., Cochonat, P., Levaché, D., Sermondadaz, G., and Seranne, M., 2006a,
233 Evidences of early to late fluid migration from an upper Miocene turbiditic channel revealed
234 by 3D seismic coupled to geochemical sampling within seafloor pockmarks, Lower Congo
235 Basin: Marine and Petroleum Geology, v. 23, no. 3, p. 387–399,
236 doi:10.1016/j.marpetgeo.2006.02.004.
- 237 Gay, A., Lopez, M., Ondréas, H., Charlou, J.L., Sermondadaz, G., and Cochonat, P., 2006b,
238 Seafloor facies related to upward methane flux within a Giant Pockmark of the Lower
239 Congo Basin: Marine Geology, v. 226, p. 81–95, doi:10.1016/j.margeo.2005.09.011.
- 240 Gay, A., Lopez, M., Berndt, C., and Séranne, M., 2007, Geological controls on focused fluid
241 flow associated with seafloor seeps in the Lower Congo Basin: Marine Geology, v. 244,
242 p. 68–92, doi:10.1016/j.margeo.2007.06.003.
- 243 Harrington, P., 1985, Formation of pockmarks by pore-water escape: Geo-Marine Letters, v. 5,
244 p. 193–197, doi:10.1007/BF02281638.
- 245 Hovland, M., 2002, On the self-sealing nature of marine seeps: Continental Shelf Research,
246 v. 22, p. 2387–2394, doi:10.1016/S0278-4343(02)00063-8.
- 247 Hovland, M., Judd, A.G., and King, L.H., 1984, Characteristic features of pockmarks on the
248 North Sea Floor and Scotian Shelf: Sedimentology, v. 31, p. 471–480, doi:10.1111/j.1365-
249 3091.1984.tb01813.x.

- 250 Hovland, M., Gardner, J.V., and Judd, A.G., 2002, The significance of pockmarks to
251 understanding fluid flow processes and geohazards: *Geofluids*, v. 2, p. 127–136,
252 doi:10.1046/j.1468-8123.2002.00028.x.
- 253 Hovland, M., Svensen, H., Forsberg, C.F., Johansen, H., Fichler, C., Fosså, J.H., Jonsson, R., and
254 Rueslåtten, H., 2005, Complex pockmarks with carbonate-ridges off mid-Norway: Products
255 of sediment degassing: *Marine Geology*, v. 218, p. 191–206,
256 doi:10.1016/j.margeo.2005.04.005.
- 257 Hovland, M., Heggland, R., De Vries, M.H., and Tjelta, T.I., 2010, Unit-pockmarks and their
258 potential significance for predicting fluid flow: *Marine and Petroleum Geology*, v. 27, p.
259 1190–1199, doi:10.1016/j.marpetgeo.2010.02.005.
- 260 Judd, A.G., and Hovland, M., 2007, *Seabed Fluid Flow: The Impact of Geology, Biology and the*
261 *Marine Environment*: Cambridge, UK, Cambridge University Press, 492 p.
- 262 King, L.H., and MacLean, B., 1970, Pockmarks on the Scotian Shelf: *Geological Society of*
263 *America Bulletin*, v. 81, p. 3141–3148, doi:10.1130/0016-
264 7606(1970)81[3141:POTSS]2.0.CO;2.
- 265 Le Gal, L., and Edy, C., 1997, CARAIBES: An integrated software for multibeam echosounder
266 and sidescan sonar data mapping, *in OCEANS '97: MTS/IEEE Conference Proceedings*, p.
267 1242–1245.
- 268 Luff, R., and Wallmann, K., 2003, Fluid flow, methane fluxes, carbonate precipitation and
269 biogeochemical turnover in gas hydrate-bearing sediments at Hydrate Ridge, Cascadia
270 Margin: Numerical modeling and mass balances: *Geochimica et Cosmochimica Acta*, v. 67,
271 p. 3403–3421, doi:10.1016/S0016-7037(03)00127-3.

- 272 MacDonald, I.R., Guinasso, N.L., Sassen, R., Brooks, J.M., Lee, L., and Scott, K.T., 1994, Gas
273 hydrate that breaches the sea floor on the continental slope of the Gulf of Mexico: *Geology*,
274 v. 22, p. 699–702, doi:10.1130/0091-7613(1994)022<0699:GHTBTS>2.3.CO;2.
- 275 Mackenzie, A.S., and Quigley, T.M., 1988, Principles of Geochemical Prospect Appraisal:
276 American Association of Petroleum Geologists Bulletin, v. 72, p. 399–415.
- 277 Marcon, Y., Sahling, H., and Bohrmann, G., 2013a, LAPM: A tool for underwater large-area
278 photo-mosaicking: *Geoscientific Instrumentation: Methods and Data Systems*, v. 2, p. 189–
279 198, doi: 10.5194/gi-2-189-2013.
- 280 Marcon, Y., Sahling, H., Allais, A.G., Bohrmann, G., and Olu-Le Roy, K., 2013b, Distribution
281 and temporal variation of mega-fauna at the Regab pockmark (Northern Congo Fan), based
282 on a comparison of videomosaics and GIS analyses: *Marine Ecology*,
283 doi:10.1111/maec.12056.
- 284 Olu-Le Roy, K., Caprais, J.C., Fifis, A., Fabri, M.C., Galéron, J., Budzinsky, H., Le Ménach, K.,
285 Khripounoff, A., Ondréas, H., and Sibuet, M., 2007, Cold-seep assemblages on a giant
286 pockmark off West Africa: Spatial patterns and environmental control: *Marine Ecology*
287 (Berlin), v. 28, p. 115–130, doi:10.1111/j.1439-0485.2006.00145.x.
- 288 Ondréas, H., and 13 others, 2005, ROV study of a giant pockmark on the Gabon continental
289 margin: *Geo-Marine Letters*, v. 25, p. 281–292, doi:10.1007/s00367-005-0213-6.
- 290 Pierre, C., and Fouquet, Y., 2007, Authigenic carbonates from methane seeps of the Congo deep-
291 sea fan: *Geo-Marine Letters*, v. 27, p. 249–257, doi:10.1007/s00367-007-0081-3.
- 292 Pierre, C., Blanc-Valleron, M.M., Demange, J., Boudouma, O., Foucher, J.P., Pape, T., Himmler,
293 T., Fekete, N., and Spiess, V., 2012, Authigenic carbonates from active methane seeps

294 offshore southwest Africa: *Geo-Marine Letters*, p. 501–513, doi:10.1007/s00367-012-0295-

295 x.

296 Sahling, H., Bohrmann, G., Spiess, V., Bialas, J., Breitzke, M., Ivanov, M., Kasten, S., Krastel,

297 S., and Schneider, R., 2008, Pockmarks in the Northern Congo Fan area, SW Africa:

298 *Complex seafloor features shaped by fluid flow: Marine Geology*, v. 249, p. 206–225,

299 doi:10.1016/j.margeo.2007.11.010.

300 Serié, C., Huuse, M., and Schødt, N.H., 2012, Gas hydrate pingoes: Deep seafloor evidence of

301 focused fluid flow on continental margins: *Geology*, v. 40, p. 207–210,

302 doi:10.1130/G32690.1.

303 Sultan, N., Marsset, B., Ker, S., Marsset, T., Voisset, M., Vernant, A.M., Bayon, G., Cauquil, E.,

304 Adamy, J., Colliat, J.L., and Drapeau, D., 2010, Hydrate dissolution as a potential

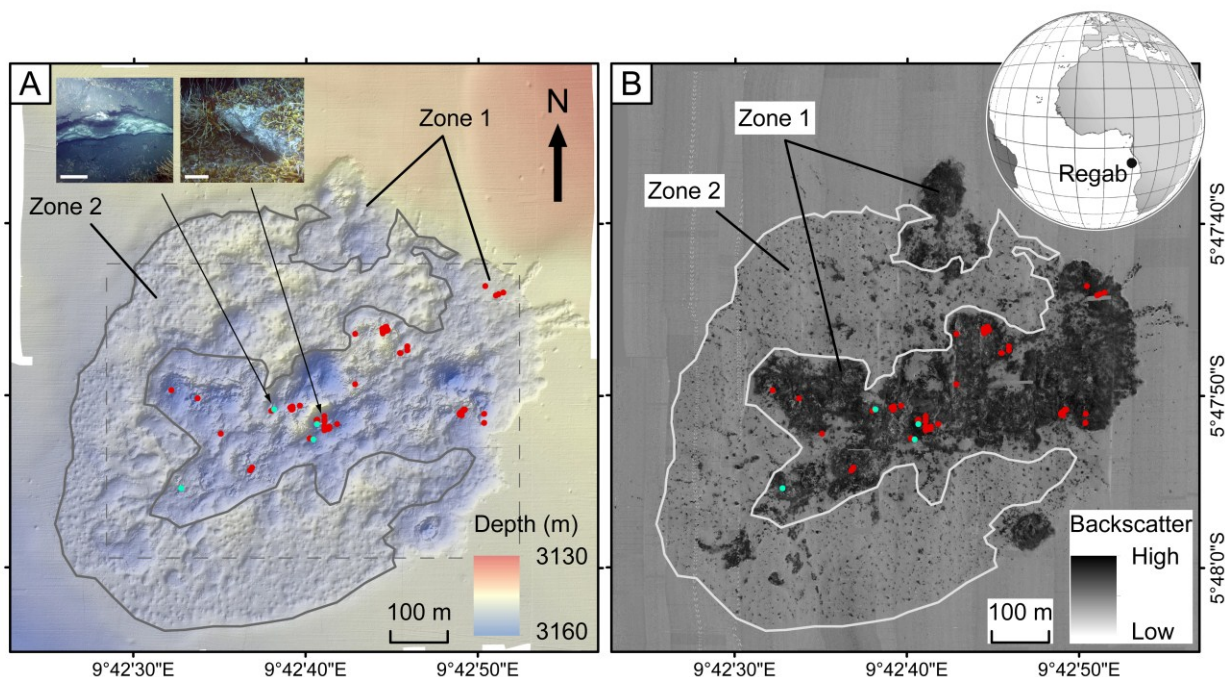
305 mechanism for pockmark formation in the Niger delta: *Journal of Geophysical Research*,

306 v. 115, B08101, doi:10.1029/2010JB007453.

307

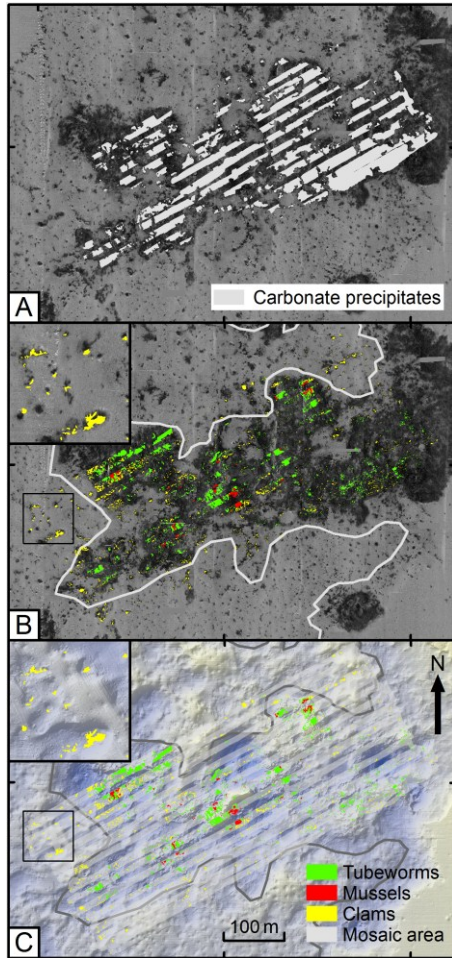
308

309 **FIGURE CAPTIONS**



310
311 Figure 1. (A) Micro-bathymetry and (B) backscatter intensity of the Regab pockmark. Seabed
312 gas emissions (red dots) were identified from both sidescan and video data. Gas hydrate outcrops
313 (blue dots) were identified from video data only. The globe view shows the location of the Regab
314 pockmark. The image insets show hydrate outcrops under broken/tilted carbonate blocks,
315 mussels and tubeworms (scale bar represents 50 cm). Zone 1 is characterized by a rugged surface
316 with large (>20 m) and deep (>3 m) depressions, strong backscatter signature, gas emissions and
317 gas hydrates at outcrop; zone 2 has a smoother appearance with comparatively low backscatter
318 signature; it is scattered by numerous (>1000) shallow (<3 m) depressions, however, gas
319 emission sites and hydrate outcrops have not been observed. The dashed rectangle in A shows
320 the extent of Figure 2.

321



322

323

324

325

326

327

328

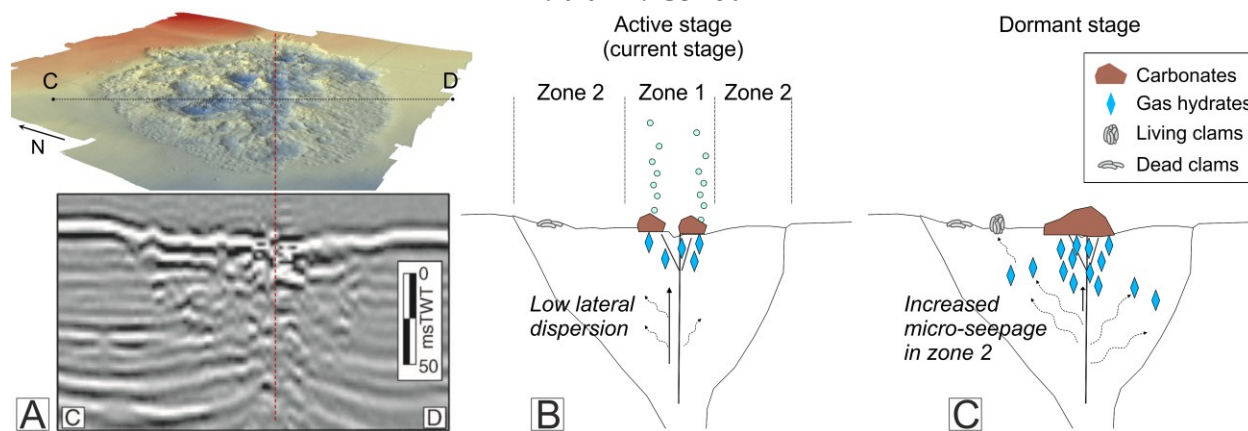
329

330

331

332

Figure 2. A: Carbonate distribution and backscatter in the center of Regab; the carbonate precipitates cause most high-backscatter anomalies. B: Fauna distribution and backscatter; tubeworms and mussels occur in areas where high-backscatter is caused by carbonate precipitates; clam shells generate high-backscatter anomalies unrelated to precipitates. C: Fauna distribution and micro-bathymetry; tubeworms and mussels occur mainly on elevated areas; clams are present in lower areas, but rarely in the deepest depressions. B and C: Inserts represent magnifications of the same area (black rectangles) of zone 2. The mosaic was constructed with the LAPM tool (Marcon et al., 2013a) by geo-referencing individual images with the ROV navigation data.



333
334 Figure 3. Plumbing system of Regab. A: The surficial fracture expression of zone 1 is located
335 right above the main seismic chimney. B: Schematic of Regab in its current active stage; seepage
336 is driven along focused pathways, leading to carbonate formation, shallow hydrates, gas escape
337 and abundant fauna in zone 1. C: Given time, carbonates and hydrate deposits cause sediment
338 vertical permeability to decrease and rising fluids to redirect and spread within surrounding
339 sediments. Seismic data after Gay et al. (2006b).